Phytochemistry Letters 41 (2021) 152–157

Contents lists available at ScienceDirect

Phytochemistry Letters

journal homepage: www.elsevier.com/locate/phytol

Five new cardenolides transformed from oleandrin and nerigoside by *Alternaria eureka* 1E1BL1 and *Phaeosphaeria* sp. 1E4CS-1 and their cytotoxic activities

Çiğdem Karakoyun [a], Melis Küçüksolak [b], Eyüp Bilgi [b], Gamze Doğan [b], Yiğit Ege Çömlekçi [b], Erdal Bedir [b,*]

[a] Department of Pharmacognosy, Faculty of Pharmacy, Ege University, 35040, Izmir, Turkey
[b] Department of Bioengineering, Faculty of Engineering, Izmir Institute of Technology, 35430, Urla, Izmir, Turkey

ARTICLE INFO

Keywords:
Nerium oleander
Oleandrin
Nerigoside
Microbial biotransformation
Endophytic fungi
Cytotoxicity

ABSTRACT

Biotransformation of oleandrin (**1**) and nerigoside (**2**) by endophytic fungi; *Alternaria eureka* 1E1BL1 and *Phaeospheria* sp. 1E4CS-1, has led to the isolation of five new metabolites (**3**, **5**, **6**, **7** and **8**) together with a known compound (**4**). The structures of the biotransformation products were elucidated by 1D-, 2D NMR and HR-MS. *Phaeospheria* sp. mainly provided monooxygenation reactions on the A and B rings, whereas *A. eureka* afforded both monooxygenated and desacetylated derivatives of the substrates. Cytotoxic activity of the compounds was tested against a non-cancerous (HEK-293) and four cancer (PANC-1, MIA PaCa-2, DU 145 and A549) cell lines by MTT cell viability assay. All compounds were less cytotoxic than oleandrin, which had IC_{50} values ranging between 2.7 and 41.9 nM. Two of the monohydroxylated metabolites, viz. 7(β)-hydroxy oleandrin (**3**) and 1(β)-hydroxy oleandrin (**7**), were also potent with IC_{50} values from 18.45 to 39.0 nM, while desacetylated + monohydroxylated, or dihydroxylated products had much lower cytotoxicity. Additionally, the lesser activity of **2** and its metabolite (**6**) possessing diginose as sugar residue inferred that oleandrose moiety is important for the toxicity of oleandrin as well as hydrophobicity of the steroid core.

1. Introduction

Biotransformation utilizes whole cell or enzyme systems as catalysts to modify substrates biochemically. Especially, the ability of microorganisms to produce high biomass, diverse enzyme systems, and catalysis of chemo/regio/enantio-selective reactions are driving factors for the application of biotransformation studies in molecular modifications. Biotransformation has become an important tool not only in the synthesis of drug molecules but also in estimating mammalian metabolism of xenobiotics and widening chemical libraries for bioactivity studies (Borges et al., 2009; Pimentel et al., 2011).

Nerium oleander L. is a medicinal and highly poisonous plant that grows in temperate regions including Mediterranean countries (Fernandes et al., 2003). The extracts prepared from the plant has diuretic and cardiotonic effects. Therefore, it has been used in the treatment of heart failure in Russia and China. It is also known to be used for the treatment of asthma, eczema, calluses, subcutaneous diseases, epilepsy, shingles, malaria, ringworm, warts, leprosy and eye diseases (Benson et al., 2015). The leaves of *N. oleander* L. comprise two major groups of secondary metabolites, cardiac glycosides and flavonoids (Siddiqui et al., 2012). Bioactivities of *N. oleander* are mostly attributed to its cardiac glycosides (Cao et al., 2018; Wen et al., 2016). Oleandrin (**1**), a well-known member of this group, is a potent inhibitor of Na^+/K^+ pump, and its excessive cytotoxic activities versus human tumor cell lines are well documented (Ko et al., 2018; Schneider et al., 2017). Unfortunately, low bioavailability and cardiotoxicity are major factors limiting clinical use of oleandrin. However, two *N. oleander* preparations (Anvirzel™: water extract, and PBI-05204: supercritical CO_2 extract) possessing oleandrin as the active constituent underwent clinical trials on advanced solid tumor patients (Schneider et al., 2017). Most recently, Plante et al. (2020) reported that the prophylactic administration of low oleandrin concentrations showed potent antiviral activity against SARS-CoV-2 with an 800-fold reduction in virus production, and >3000-fold reduction in infectious virus production in Vero cells, putting oleandrin on a spotlight once more (Plante et al., 2020).

Although oleandrin is an important natural product with potent

* Corresponding author.
E-mail address: erdalbedir@iyte.edu.tr (E. Bedir).

https://doi.org/10.1016/j.phytol.2020.12.003
Received 2 September 2020; Received in revised form 30 November 2020; Accepted 2 December 2020
Available online 24 December 2020

biological activities, only a few structure-activity relationship studies (SARs) are reported. These studies were mainly focused on the modification at C-4′ on the sugar residue (oleandrose) because of the modification difficulties on the aglycone (oleandrigenin). Moreover, there has been no microbial biotransformation study on oleandrin to give clue regarding its possible mammalian metabolites. Therefore, it is essential to perform further SAR studies on anti-proliferative activity of oleandrin with more analogues, as well it is critical to shed light on its metabolism.

As part of our current studies on the modification of active natural products (Ekiz et al., 2019; Özçınar et al., 2018), we herein report a series of oleandrin metabolites, obtained via fungal biotransformation using *Alternaria eureka* 1E1BL1 and *Phaeosphaeria* sp. 1E4CS-1, and their cytotoxic activities versus four different human cancer (PANC-1, MIA PaCa-2, DU 145, A549) and a normal (HEK-293) cell lines. Additionally, as our substrate had 7% isomeric impurity, viz. nerigoside (**2**) possessing diginose residue instead of oleandrose in oleandrin, an additional biotransformation product was obtained contributing to interpretation of SARs.

2. Results and discussion

The main substrate, oleandrin (**1**), was isolated from dried leaves of *N. oleander* (14 kg) using a previously described method (Ryer and Marie, 1948) with minor modifications. However, oleandrin (**1**) (4 g), was isolated with 93 % purity as admixture with its isomer, nerigoside (**2**) (%7).

A preliminary screening study was performed to designate the most potent fungi with ability to transform the substrate into varied metabolites. A thin layer chromatography analysis was carried out to monitor the biotransformation products using fifteen microorganisms (*Camarosporium laburnicola* 1E4BL1, undefined species NOR4, *Alternaria eureka* 1E1BL1, *Penicillium* sp. 1E4BR2-2, *Alternaria alternata* 1E2L1, *Podospora* sp. 1E4CR-1, *Penicillium roseopurpureum* 1E4BS1, *Fusarium* sp. 1E4AS-1, *Fusarium* sp. 1E4CS, *Fusarium torulosum* 1E2L-1, *Cunninghamella blakesleeana* NRRL1369, *Phaeosphaeria* sp. 1E4CS-1, *Neosartorya hiratsukae* 1E2AR1-1, *Fusarium acuminatum* 1E3AS1-1, and *Allophaeosphaeria cytisi* 1E4AL*) via analytical-scale experiments. Among the screened fungi, *Alternaria eureka* 1E1BL1 and *Phaeosphaeria* sp. 1E4CS-1 were selected for further preparative-scale studies that afforded six metabolites (**3**-**8**) (see Fig. 1).

The biotransformation studies with the endophytic fungus *A. eureka* for 14 days afforded three previously-undescribed metabolites (**3**, **5** and **6**) together with a known compound, desacetyl oleandrin (**4**) (Abe et al., 1996).

The molecular formula of **3** was determined as $C_{32}H_{48}O_{10}$ based on the major ion peak at *m/z* 615.31494 $[M + Na]^+$ (calcd. 615.31452 for $C_{32}H_{48}NaO_{10}$). An increase of sixteen amu (atomic mass unit) compared to **1** suggested that **3** was a monooxygenated metabolite of the substrate. The ^{13}C and ^{1}H resonances of **3** deriving from the sugar residue (oleandrose) were identical to those of **1**, revealing that the hydroxylation occurred on the oleandrigenin nucleus. In the ^{1}H NMR spectrum, an additional oxymethine signal at δ_H 3.87 was observed corresponding to a carbon δ_C 71.2 in the HSQC spectrum. The ^{13}C NMR spectrum of **3** showed that C-6 (δ_C 37.4) and C-8 (δ_C 46.4) signals underwent a significant down-field shift (*ca.* 10.8 and 4.5 ppm, respectively) when compared to **1**, suggesting an oxygenation at C-7 position. In the COSY spectrum, identification of the spin system starting from the H-8 [H-8 (δ_H 1.72 m) → H-7 (δ_H 3.87 m) → H-6 (δ_H 1.47 m, 1.91 d, J = 2.9 Hz)], together with the long range correlations from C-7 to H-6 and H-8, and from C-14 to H-7 in the HMBC spectrum verified the location of transformation. The relative configuration was established via 2D-NOESY data, in which strong correlation of H-7 with the α-oriented H-15, which was assigned based on its correlation with H-16α, revealed that the hydroxy group at C-7 was β-oriented (Fig. 2). Consequently, the structure of **3** was determined as 7(β)-hydroxyoleandrin.

The HR-ESI-MS of **5** exhibited a sodium adduct ion at *m/z* 573.30479 $[M + Na]^+$ ($C_{30}H_{46}NaO_9$, calcd. 573.30395), supporting a molecular formula of $C_{30}H_{46}O_9$ with eight indices of hydrogen deficiency (HD). In the ^{1}H and ^{13}C NMR spectra, the absence of carbonyl and upfield methyl signals of the acetoxy group clarifying the decrease in HD, together with the upfield shift of H-16 (*ca.* 1 ppm) indicated a desacetylation at C-16. A broad singlet signal observed at δ_H 3.94, corresponding to a carbon at δ_C 70.6 in the HSQC spectrum, indicated an additional oxymethine group in the structure. Examination of the COSY spectrum suggested oxygenation at C-7, as in **3**. The HMBC correlations of H-7 with C-14, of H-6 with C-7 and of H-8 with C-7 were supportive of the proposed structure. Inspection of the 2D-NOESY spectrum of **5** and superimposable ^{1}H and ^{13}C NMR data with those of **3** in the B ring provided evidence for the β-orientation of the hydroxy group at C-7. Thus, the new metabolite was characterized as 7(β)-hydroxy,16-desacetyloleandrin.

Compound **6** gave a molecular formula $C_{30}H_{46}O_9$ based on the HR-ESI-MS analysis (*m/z* 573.30489 $[M + Na]^+$, $C_{30}H_{46}NaO_9$, calcd. 573.30395). The absence of characteristic acetyl group resonances in the ^{1}H and ^{13}C NMR spectra was readily noted. The ^{13}C and ^{1}H NMR data substantiated with the ^{1}H,^{1}H-COSY, HSQC and HMBC spectra revealed that the resonances arising from the steroid backbone were identical with those of **5** except for the sugar signals. The downfield shift of the anomeric carbon signal (ca. 1.2 ppm), together with the upfield shift of C-2″ (δ_C 31.6) and C-4″ (δ_C 67.9) in comparison to **5** were evident for the presence of a different sugar unit. Thus, on the basis of the proton and carbon chemical shifts, multiplicity of the signals and absolute values of coupling constants, the sugar residue was identified as β-diginosyl indicating that the transformed substrate was nerigoside (**2**). Thus, the structure of **6** was elucidated as 7(β)-hydroxy,16-desacetylnerigoside.

The incubation of **1** and **2** with *Phaeosphaeria* sp. for 18 days yielded two new metabolites (**7** and **8**).

The HR-ESI-MS data of **7** (*m/z* 615.31600 $[M + Na]^+$, calcd. for $C_{32}H_{48}NaO_{10}$ 615.31452) supported a molecular formula $C_{32}H_{48}O_{10}$, implying a monohydroxylation. In the ^{1}H and ^{13}C spectra, resonances of oleandrose, acetoxy, butyrolactone, and the C-14 oxymethine carbon in the low-field displayed no significant discrepancy compared to **1**. The signal observed at δ_H 3.70 suggested another oxymethine group corresponding to a carbon at δ_C 72.5 in the HSQC spectrum. A detailed

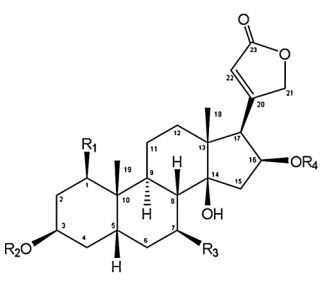

Compound		R_1	R_2	R_3	R_4
Oleandrin	1	H	L-oleandrosyl	H	$COCH_3$
Nerigoside	2	H	D-diginosyl	H	$COCH_3$
	3	H	L-oleandrosyl	OH	$COCH_3$
	4	H	L-oleandrosyl	H	H
	5	H	L-oleandrosyl	OH	H
	6	H	D-diginosyl	OH	H
	7	OH	L-oleandrosyl	H	$COCH_3$
	8	OH	L-oleandrosyl	OH	$COCH_3$

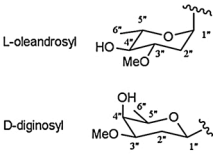

Fig. 1. Biotransformation products of oleandrin and nerigoside by *Alternaria eureka* 1E1BL1 and *Phaeosphaeria* sp. 1E4CS-1.

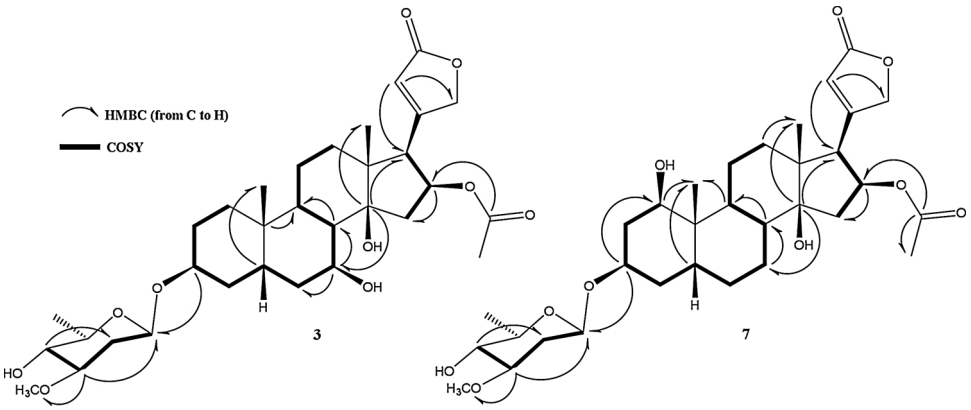

Fig. 2. Key COSY and HMBC correlations of **3** and **7**.

inspection of the ^{13}C NMR spectrum showed down-field shifts for C-2 and C-10 signals (ca. 5 ppm) and upfield shift for C-19 (ca. 5 ppm) when compared to those of **1**; therefore, a monooxygenation at C-1 was readily suggested. In the HMBC spectrum, key long-range correlations from the 72.5 ppm signal to H-19 (δ_H 1.09), and C-5 to H-1 (δ_H 3.70) substantiated that the new hydroxyl group was located at C-1. The relative configuration at C-1 was determined based on the 2D-NOESY data. The H-1 (δ_H 3.70 m) signal showed too weak NOE correlation with the β-oriented H-19, and no NOE with H-5 revealing that the hydroxy group at C-1 was β-oriented. Thus, the structure of **7** was deduced as 1 (β)-hydroxyoleandrin.

The major ion peak at *m/z* 631.31154 $[M + Na]^+$ ($C_{32}H_{48}NaO_{11}$, calcd. 631.30943) in the HR-ESI-MS spectrum of **8** displayed 32 amu increase over **1**, suggesting a dihydroxy analog. In the low-field of the ^1H NMR spectrum, two additional low-field resonances (δ_H 3.69 and δ_H 3.94) were observed. Besides, two extra down-field carbon signals at δ 72.3 and δ 71.0 were also noted. In order to deduce oxidation positions, the 2D NMR spectra were inspected in detail. Like **7**, monooxygenation at C-1 was confirmed by the HMBC spectrum, which showed a cross-peak between the 72.3 ppm signal and H-19 (δ_H 1.15). The second hydroxy group was located at C-7 on the basis of the COSY correlation of H-7 (δ_H 3.94) with H_2-6 (δ_H 1.57) and H-8 (δ_H 1.79) as in **3**. The orientation of OH-1 and OH-7 was deduced to be β based on the 2D-NOESY data, in which the presence of H-7 to H-15α and the absence of H-1 to H-5 correlations were evident. On the basis of these results, the structure of **8** was identified as 1(β),7(β)-dihydroxyoleandrin.

Cytotoxic activities of compounds **1–8** on four cancer (A549 – adenocarcinomic human alveolar basal epithelial cells, DU 145 - human prostate cancer cells, MIA-PaCa-2 - human pancreatic cancer cells and PANC-1 - human pancreatic cancer cells) and a healthy (HEK-293 - human embriyonic kidney cells) cell lines were determined via MTT cell viability analysis using four different concentrations (1 nM, 10 nM, 100 nM and 500 nM). The results were summarized in Table 3. The cytotoxicity of the compounds was compared with doxorubicin as positive control. Oleandrin showed the highest cytotoxic activity regardless of the cell type, as well it had 17- to 27-fold higher cytotoxicity than nerigoside on human cancer lines. These results were in accordance with the literature, in which it was reported that sugar unit (l-oleandrose for oleandrin and d-diginose for nerigoside) may vary the effects of cardenolides.

While increasing hydrophilicity, the monohydroxylated metabolites (**3** and **7**) were slightly less active than oleandrin with IC_{50} values between 18.45 and 39.0 nM on tumor cell lines. Increase of hydrophilicity via hydroxylation positively affects the water solubility of oleandrin and its clearance from the body; however, selectivity index (SI) of **3** and **7** was not improved meaningfully ($4.0 \leq SI \geq 7.9$) compared to oleandrin ($2.8 \leq SI \geq 15.5$) still limiting their possible use in clinic. Further increase of hydrophilicity as in **8** (1,7-dihydroxyoleandrin) resulted in loss of cytotoxicity towards tumor cells from 19.0- to 32.2-fold. In regard to desacetylated metabolites, compound **4** (desacetyloleandrin) was considerably active with IC_{50} values ranging from 20 to 98 nM (A549 and PANC-1, respectively), whereas desacetylation coupled with hydroxylation (**5** and **6**) led to substantial decrease in cytotoxicity (307.9 nM $\leq IC_{50} \geq$ 500). These results indicate that hydrophobicity, presence of 16-*O*-acetyl group and type of sugar unit are important structural features defining cytotoxic activities of cardiac glycosides.

In conclusion, this is the first report on biotransformation of oleandrin and nerigoside affording five new metabolites, which are of significant for estimating possible mammalian metabolites. Moreover, preparation of further derivatives via biotransformation are warranted to make thorough structure activity relationship deductions that may allow to find safer molecules with higher therapeutic window.

3. Experimental

3.1. General procedures

IR spectra were obtained on Perkin Elmer Spectrum 100 FT-IR spectrometer. The general experimental procedures were described previously for NMR, HR-ESI-MS, optical rotations and chromatographic studies (Ekiz et al., 2019).

3.2. Plant material and starting compounds (1 and 2)

Nerium oleander was collected from Urla, Izmir, Turkey in Nov 2019 (38°19′09.4″N 26°38′35.5″E). The plant was confirmed by Prof. Dr. Erdal Bedir (Deparment of Bioengineering, IZTECH, Izmir, Turkey). Voucher specimens have been deposited at the Herbarium of the Department of Pharmacognosy, Faculty of Pharmacy, Ege University, Izmir, Turkey with the number of 1640.

Admixture of oleandrin (**1**) and nerigoside (**2**) (93:7) was isolated from dried leaves of *Nerium oleander* using a modified method of oleandrin extraction procedure described in literature (Ryer and Marie, 1948).

3.3. Microorganisms

The endophytic fungi *Alternaria eureka* 1E1BL1 and *Phaeosphaeria* sp. 1E4CS-1 were isolated from *Astragalus* species (Ekiz, 2016; Ekiz et al., 2019). All cultures were maintained on potato dextrose agar (PDA) slants and stored at 4 °C until use. Prior to biotransformation, the fungus was precultivated on PDA in Petri dishes for 10 days at 25 °C.

3.4. Microbial transformation procedure

The microbial biotransformation processes of analytical and preparative scales were carried out as described previously (Ekiz et al., 2019). Preparative-scale biotransformation studies were performed employing 1500 mg of **1** with *A. eureka* for 14 days and 1000 mg of **1** with *Phaeosphaeria* sp. for 18 days (25 °C and 180 rpm).

3.5. Extraction and isolation

After an incubation period, the fungal mycelia were filtered on a Buchner funnel, and the filtrate was extracted with EtOAc (×3). The organic phase was evaporated under reduced pressure to dryness. Compounds **3**– **7** were isolated from the EtOAc extract (2.37 g) of the biotransformation media of the admixture of **1** and **2** with *A. eureka*. This extract was chromatographed initially on a silica gel column (180 g) eluted with $CHCl_3$:MeOH (98:2, 97:3, 96:4, 90:10) to give 8 main fractions (A – H). Fraction B (114.3 mg) was applied to VLC (vacuum-liquid chromatography) loaded with reversed-phase silica gel (RP-C18, 15 g), using a MeOH:H_2O (65:35), to give metabolites **3** (13.5 mg). Fraction D (135.9 mg) was subjected to VLC using reversed-phase silica gel (RP-C18, 15 g) and eluted with MeOH:H_2O (60:40), which provided 15 fractions (D1-15). Fractions D10-D15 were combined to afford metabolite **4** (8 mg). Fraction F (90.4 mg) was applied to VLC (vacuum-liquid chromatography) loaded with reversed-phase silica gel (RP-C18, 15 g), using a MeOH:H_2O gradient (50:50, 60:40) to give 30 fractions. Fractions F21-F30 (46.3 mg) were subjected to a preparative thin layer chromatography employing with *n*-hexane:EtOAc:MeOH (10:10:3.5) to obtain **5** (25 mg). Fraction E (64.9 mg) was chromatographed on a silica gel column (30 g) eluted with *n*-hexane:EtOAc:MeOH gradient (10:10:0.25, 10:10:0.5, 10:10:1) to give 123 fractions (E1-123). Fractions E98-E123 were combined and subjected to Sephadex LH-20 column chromatography (7.9 mg) and eluted with MeOH, which provided 50 fractions. Fractions 40–44 were pooled together and 3.1 mg of **6** was obtained.

Compounds **7** – **8** were isolated from the EtOAc extract (281 mg) of *Phaeosphaeria* sp. and the admixture of **1** and **2**. The EtOAc extract was subjected to VLC loaded with reversed-phase silica gel (RP-C18, 35 g) to yield **7** (11.1 mg), **3** (4.9 mg) and one impure fraction (A) after elution with ACN/H_2O (30:70). Fraction A (10 mg) was further chromatographed using a silica gel column and eluted with *n*-hexane:EtOAc:MeOH (10:10:0.1) to afford **8** (1.8 mg).

3.6. Compound characterization

Compound **1** (*Oleandrin*: *3β-O-(α-L-Oleandrosyl)-16β-acetoxy-14β-hydroxy-5β,14β-card-20(22)-enolide*): FT-IR ($CHCl_3$): 3491, 2935, 1738, 1451, 1379, 1248, 1106, 1034, 999 cm^{-1}. HR-ESI-MS (positive ion mode): *m/z* 599.32081 $[M + Na]^+$ ($C_{32}H_{48}NaO_9$, calcd. 599.31960). $[\alpha]^{29}_D$ = -28.2 (c 0.39, MeOH).^{1}H NMR ($CDCl_3$, 400 MHz) and ^{13}C NMR ($CDCl_3$, 100 MHz): see Table S1.

Compound **2** (*Nerigoside*: *3β-O-(β-D-Diginosyl)-16β-acetoxy-14β-hydroxy-5β,14β-card-20(22)-enolide)*: FT-IR ($CHCl_3$): 3488, 2979, 2937, 2897, 1736, 1451, 1381, 1247, 1171, 1097, 1035, 757 cm^{-1}. HR-ESI-MS (positive ion mode): *m/z* 599.32033 $[M + Na]^+$ ($C_{32}H_{48}NaO_9$, calcd. 599.31960). $[\alpha]^{29}_D$ = -7.1 (c 0.14, MeOH). ^{1}H NMR ($CDCl_3$, 400 MHz) and ^{13}C NMR($CDCl_3$, 100 MHz): see Table S1.

Compound **3** (*3β-O-(α-L-Oleandrosyl)-16β-acetoxy-7β,14β-dihydroxy-5β,14β-card-20(22)-enolide*): FT-IR ($CHCl_3$): 3420, 2934, 1738, 1457, 1382, 1245, 1107, 1030 cm^{-1}. HR-ESI-MS (positive ion mode): *m/z* 615.31494 $[M + Na]^+$ ($C_{32}H_{48}NaO_{10}$, calcd. 615.31452). $[\alpha]^{29}_D$ = -15.8 (c 0.19, MeOH). ^{1}H NMR ($CDCl_3$, 400 MHz) and ^{13}C NMR ($CDCl_3$, 100 MHz): see Tables 1 and 2.

Compound **4** (*3β-O-(α-L-Oleandrosyl)-14β,16β-dihydroxy-5β,14β-card-20(22)-enolide)*: FT-IR ($CHCl_3$): 3460, 2936, 1739, 1452, 1382, 1105, 1032, 997, 758 cm^{-1}. HR-ESI-MS (positive ion mode): *m/z* 557.30950 $[M + Na]^+$ ($C_{30}H_{46}NaO_8$, calcd. 557.30904). $[\alpha]^{29}_D$ = -4.65 (c 0.43, MeOH). ^{1}H NMR ($CDCl_3$, 400 MHz) and ^{13}C NMR ($CDCl_3$, 100 MHz): see Table S1.

Compound **5** (*3β-O-(α-L-Oleandrosyl)-7β,14β,16β-trihydroxy-5β,14β-card-20(22)-enolide)*: FT-IR ($CHCl_3$): 3404, 2973, 2934, 1736, 1456, 1383, 1106, 1032, 995, 759 cm^{-1}. HR-ESI-MS (positive ion mode): *m/z* 573.30479 $[M + Na]^+$ ($C_{30}H_{46}NaO_9$, calcd. 573.30395). $[\alpha]^{29}_D$ = 6.25 (c 0.16, MeOH). ^{1}H NMR ($CDCl_3$, 400 MHz) and ^{13}C NMR ($CDCl_3$, 100 MHz): see Tables 1 and 2.

Table 1
^{1}H NMR data of **3**, **5**, **6**, **7** and **8** (in $CDCl_3$).

	3	5	6	7	8
H	δ_H (*J* in Hz)	δ_H (*J* in Hz)	δ_H (*J* in Hz)	δ_H (*J* in Hz)	δ_H (*J* in Hz)
1	1.46 m; 2H	1.43 m, 2H	1.49 m, 2H	3.70 m	3.69 m
2	1.44 m; 1.53 m	1.36 m; 1.53 m	1.39 m; 1.69 m	1.83 m; 1.97 m	1.77 m; 1.97 m
3	3.84 m	3.84 s	3.99 m	4.17 t (2.8)	4.14 m
4	1.56 m, 2H	1.54 m, 2H	1.58 m, 2H	1.55 m; 1.74 m	1.67 m, 2H
5	1.78 m	1.75 m	1.79 m	1.92 m	2.04 d (1.5)
6	1.47 m; 1.91 d (2.9)	1.48 m; 1.91 td (12.2, 4.9)	1.50 m; 1.94 m	1.34 m; 1.84 m	1.57 m; 1.90 m
7	3.87 m	3.94 td (11.2, 5.0)	3.97 m	1.36 m; 1.77 m	3.94 m
8	1.72 m	1.70 d (11.0)	1.71 m	1.58 m	1.79 m
9	1.49 m	1.52 m	1.52 m	1.40 m	1.39 m
10	–	–	–	–	–
11	1.27 m; 1.40 m	1.22 m; 1.39 m	1.25 m; 1.41 m	1.19 m; 1.27 m	1.35 m, 2H
12	1.26 m; 1.51 m	1.23 m; 1.63 m	1.25 m; 1.64 m	1.27 m; 1.56 m	1.24 m; 1.53 m
13	–	–	–	–	–
14	–	–	–	–	–
15	1.91 d (2.9); 2.77 ddd (15.1, 9.9, 2.8)	2.04 d (13.9); 2.39 dd (14.0, 5.6)	2.06 d (13.9); 2.39 dd (13.9, 5.7)	1.78 m; 2.68 dd (15.6, 9.6)	1.94 m; 2.73 dd (15.2, 9.8)
16	5.51 td (9.3, 2.6)	4.44 t (6.2)	4.43 s	5.45 td (9.2, 2.5)	5.50 t (9.4)
17	3.26 dd (9.0, 2.8)	2.90 d (6.5)	2.92 d (6.6)	3.18 dd (10.1, 8.6)	3.26 d (8.9)
18	0.95 s	0.95 s	0.95 s	0.93 s	0.96 s
19	0.98 s	0.98 s	0.97 s	1.09 s	1.15 s
20	–	–	–	–	–
21	4.93 m; 5.13 m	4.88 dt (18.2, 1.5); 5.04 dt (18.1, 1.6)	4.89 dt (18.1, 1.7); 5.04 dt (18.1, 1.8)	4.85 dd (18.2, 1.8); 4.96 d (1.9)	4.93 dt (18.6, 1.7); 5.12 m
22	5.91 dd (3.3, 1.7)	5.97 d (1.6)	5.97 s	5.97 d (1.8)	5.92 d (1.8)
23	–	–	–	–	–
1′	–	–	–	–	–
2′	1.96 s	–	–	1.96 s	2.04 s
1″	4.94 m	4.94 d (3.5)	4.69 m	5.00 dd (4.2, 2.8)	4.99 d (3.6)
2″	1.49 m; 2.20 dt (13.0, 3.7)	1.48 m; 2.20 dd (12.6, 4.7)	1.77 m; 1.83 m	1.57 m; 2.19 dd (12.9, 4.9)	1.57 m; 2.19 m
3″	3.50 m	3.51 m	3.58 d (3.2)	3.47 s	3.43 m
4″	3.15 td (9.1, 2.8)	3.14 td (9.1, 1.3)	3.40 s	3.16 dd (10.1, 8.6)	3.17 t (9.2)
5″	3.69 ddd (9.3, 6.2, 2.9)	3.68 m	3.91 d (6.6)	3.73 m	3.71 m
6″	1.26 m	1.24 dd (6.3, 1.2)	1.23 m	1.29 d (6.3)	1.28 m
3″OCH$_3$	3.39 s	3.39 s	3.39 s	3.38 s	3.38 s

Table 2
^{13}C NMR data of **3**, **5**, **6**, **7** and **8** (in $CDCl_3$).

C	3 δ_C (ppm)	5 δ_C (ppm)	6 δ_C (ppm)	7 δ_C (ppm)	8 δ_C (ppm)
1	30.1 t	30.1 t	29.9 t	72.5 d	72.3 d
2	26.5 t	26.5 t	26.6 t	31.7 t	31.4 t
3	71.0 d	70.9 d	72.3 d	71.0 d	70.6 d
4	31.1 t	30.9 t	31.3 t	28.1 t	29.3 t
5	37.5 d	37.4 d	37.3 d	30.4 d	31.8 t
6	37.4 t	36.9 t	37.2 t	26.0 t	36.9 t
7	71.2 d	70.6 d	71.1 d	20.8 t	71.0 d
8	46.4 d	46.2 d	46.5 d	41.9 d	46.6 d
9	35.1 d	35.2 d	35.0 d	37.6 d	37.2 d
10	35.2 s	34.9 s	35.2 s	40.2 s	40.1 s
11	20.8 t	21.4 t	21.4 t	20.8 t	20.5 t
12	38.8 t	41.9 t	42.0 t	39.2 t	38.7 t
13	50.1 s	49.5 s	49.4 s	49.9 s	49.9 s
14	83.8 s	86.6 s	86.6 s	84.1 s	83.7 s
15	42.5 t	42.3 t	42.4 t	41.3 t	42.6 t
16	74.1 d	73.5 d	73.7 d	73.9 d	74.0 d
17	56.6 d	58.4 d	58.6 d	56.0 d	56.5 d
18	16.1 q	17.0 q	17.0 q	16.1 q	16.3 q
19	23.9 q	23.9 q	23.7 q	18.9 q	18.9 q
20	167.9 s	169.3 s	169.0 s	167.8 s	168.5 s
21	76.2 t	75.7 t	75.5 t	75.8 t	76.1 t
22	121.5 d	119.9 d	119.7 d	121.5 d	121.8 d
23	174.4 s	174.9 s	174.6 s	174.2 s	174.3 s
1′	170.7 s	–	–	170.6 s	170.7 s
2′	21.2 q	–	–	21.2 q	21.2 q
1″	95.6 d	95.6 d	96.8 d	93.9 d	94.1d
2″	34.6 t	34.6 t	31.6 t	34.3 t	34.2 t
3″	78.5 d	78.5 d	78.6 d	78.2 d	78.2 d
4″	76.3 d	76.3 d	67.9 d	76.1 d	76.1 d
5″	67.8 d	67.8 d	69.2 d	68.3 d	68.4 d
6″	18.0 q	17.9 q	16.7 q	18.0 q	18.0 q
3″OCH_3	56.6 q	56.5 q	57.3 q	56.8 q	56.9 q

Table 3
Cytotoxic Activities of **1-8**.

Compound	A549	DU 145	PANC-1	MIA-PaCa-2	HEK-293
1	2.7	7.92	15.05	9.10	41.9
2	46.75	208.5	339.4	246.5	473
3	18.45	19.4	28	26.90	146.5
4	20	42.85	98	53.75	379.5
5	307.9	477.1	>500	>500	>500
6	459.5	>500	>500	>500	>500
7	20	28.15	39	27.75	156
8	51.4	250.5	335.9	292.75	>500
Doxorubicin	>500	>500	>500	>500	197.2

IC_{50} values are the concentration (nM) required 50 % cell viability inhibition for a given compound with a 48 h treatment and were calculated using cell viability (%) formula via nonlinear regression analysis. Measurement was carried out in triplicate. IC_{50} values were given for A549 human lung cancer cell line, DU145 human prostate cancer cell line, PANC-1 human pancreatic cancer cell line, MIA-PaCa-2 pancreatic cancer cell line and HEK-293 human embriyonic kidney cell line. Doxorubicin was used as control.

Compound **6** (*3β-O-(β-D-Diginosyl)-7β,14β,16β-trihydroxy-5β,14β-card-20(22)-enolide*): FT-IR ($CHCl_3$): 3654, 3426, 2980, 2892, 1736, 1463, 1382, 1163, 1094, 958, 775 cm^{-1}. HR-ESI-MS (positive ion mode): *m/z* 573.30489 $[M + Na]^+$ ($C_{30}H_{46}NaO_9$, calcd. 573.30395). $[\alpha]^{29}_D = 4.76$ (c 0.21, MeOH). ^1H NMR ($CDCl_3$, 400 MHz) and ^{13}C NMR ($CDCl_3$, 100 MHz): see Tables 1 and 2.

Compound **7** (*3β-O-(α-L-Oleandrosyl)-16β-acetoxy-1β,14β-dihydroxy-5β,14β-card-20(22)-enolide*): FT-IR ($CHCl_3$): 3491, 2980, 1740, 1457, 1379, 1248, 1151, 1054, 992, 957, 774 cm^{-1}. HR-ESI-MS (positive ion mode): *m/z* 615.31600 $[M + Na]^+$ ($C_{32}H_{48}NaO_{10}$, calcd. 615.31452). $[\alpha]^{29}_D$ = -16.67 (c 0.24, MeOH). ^1H NMR ($CDCl_3$, 400 MHz) and ^{13}C NMR ($CDCl_3$, 100 MHz): see Tables 1 and 2.

Compound **8** (*3β-O-(α-L-Oleandrosyl)-16β-acetoxy-1β,7β,14β-trihydroxy-5β,14β-card-20(22)-enolide*): FT-IR ($CHCl_3$): 3655, 3451, 2980, 2894, 1741, 1473, 1383, 1253, 1156, 1087, 967, 775 cm^{-1}. HR-ESI-MS (positive ion mode): *m/z* 631.31154 $[M + Na]^+$ ($C_{32}H_{48}NaO_{11}$, calcd. 631.30943). $[\alpha]^{29}_D$ = -16.67 (c 0.18, MeOH). ^1H NMR ($CDCl_3$, 400 MHz) and ^{13}C NMR ($CDCl_3$, 100 MHz): see Tables 1 and 2.

3.7. MTT assay

HEK-293 (human embryonic kidney), PANC-1 (human pancreatic cancer), MIA PaCa-2 (human pancreatic cancer), DU 145 (human prostate cancer) and A549 (adenocarcinomic human alveolar basal epithelial) cell lines were used to determine IC_{50} values of elucidated molecules. EMEM (Eagle's minimal essential medium) was used for HEK-293 and DMEM-HG (Dulbecco's modified Eagle Medium- high glucose) was used other cell lines, both media were supplemented with 10 % FBS and 1% L-glutamine. Cells, which were incubated at 37 °C in 5% CO_2 atmosphere till to the reach approximately 85 % confluency, were passaged, and after 24 h of incubation, cells were inoculated with the density of 6000 cells/well onto 96 well plate for PANC-1 and 5000 cells/well for other cell lines. Molecules dissolved in DMSO were subjected to cells with the concentrations of 1, 10, 100, and 500 nM. Oleandrin and doxorubicin were used as controls for comparison.

Cellular viability was assessed via MTT assay after exposure to molecules. After treatment of 24 h, the culture medium removed from each well and replaced with medium supplemented with 10 % MTT solution and incubated at 37 °C in 5% CO_2 atmosphere for 3 h. At the end of incubation period, reduced tetrazolium salts (formazan crystals after reduction via mitochondrial succinate dehydrogenase) were solubilized in DMSO, absorbance of each well measured with microplate reader at 570 nm.

Cell viability (%) was determined as follows:

Cell viability (%) = [(experimental absorbance-background absorbance)$_{570\ nm}$ / (DMSO control absorbance – background absorbance) $_{570\ nm}$] x100

Declaration of Competing Interest

The authors declare no conflict of interest.

Acknowledgement

This project was supported by The Scientific and Technological Research Council of Turkey (TUBITAK, Project No: 152Z118). We are thankful to Dr. Özge Özşen for her assistance in preliminary experiments.

Appendix A. Supplementary data

Supplementary material related to this article can be found, in the online version, at doi:https://doi.org/10.1016/j.phytol.2020.12.003.

References

Abe, F., Yamauchi, T., Minato, K., 1996. Presence of cardenolides and ursolic acid from oleander leaves in larvae and frass of *Daphnis nerii*. Phytochemistry 42, 45–49.
Benson, K.F., Newman, R.A., Jensen, G.S., 2015. Antioxidant, anti-inflammatory, anti-apoptotic, and skin regenerative properties of an Aloe vera-based extract of *Nerium oleander* leaves (NAE-8®). Clin. Cosmet. Investig. Dermatol. 8, 239.
Borges, W.S., Borges, K.B., Bonato, P.S., Said, S., Pupo, M.T., 2009. Endophytic fungi: natural products, enzymes and biotransformation reactions. Curr. Org. Chem. 13, 1137–1163.
Cao, Y.-L., Zhang, M.-H., Lu, Y.-F., Li, C.-Y., Tang, J.-S., Jiang, M.-M., 2018. Cardenolides from the leaves of *Nerium oleander*. Fitoterapia 127, 293–300.
Ekiz, G., 2016. Research on Bioactive Secondary Metabolite Profile of Septofusidium Berolinense and Biotranformation of Cycloartane Type Saponins by Endophytic Fungi. Department of Bioengineering. Ege University, Izmir.
Ekiz, G., Yılmaz, S., Yusufoglu, H., Kırmızıbayrak, P.B., Bedir, E., 2019. Microbial transformation of Cycloastragenol and astragenol by endophytic Fungi isolated from *Astragalus* species. J. Nat. Prod. 82, 2979–2985.

Fernandes, P., Cruz, A., Angelova, B., Pinheiro, H., Cabral, J., 2003. Microbial conversion of steroid compounds: recent developments. Enzyme Microb. Technol. 32, 688–705.
Ko, Y.S., Rugira, T., Jin, H., Park, S.W., Kim, H.J., 2018. Oleandrin and its derivative odoroside a, both cardiac glycosides, exhibit anticancer effects by inhibiting invasion via suppressing the stat-3 signaling pathway. Int. J. Mol. Sci. 19, 3350.
Özçınar, O., Tağ, O., Yusufoglu, H., Kivçak, B., Bedir, E., 2018. Biotransformation of neoruscogenin by the endophytic fungus *Alternaria eureka*. J. Nat. Prod. 81, 1357–1367.
Pimentel, M.R., Molina, G., Dionísio, A.P., Maróstica Junior, M.R., Pastore, G.M., 2011. The use of endophytes to obtain bioactive compounds and their application in biotransformation process. Biotechnol. Res. Int. 2011.
Plante, K.S., Plante, J.A., Fernandez, D., Mirchandani, D., Bopp, N., Aguilar, P.V., Sastry, K.J., Newman, R.A., Weaver, S.C., 2020. Prophylactic and Therapeutic Inhibition of *In Vitro* SARS-CoV-2 Replication by Oleandrin. bioRxiv.
Ryer, A.I., Marie, F., 1948. Process for the Isolation of Oleandrin. Google Patents.
Schneider, N.F.Z., Cerella, C., Simões, C.M.O., Diederich, M., 2017. Anticancer and immunogenic properties of cardiac glycosides. Molecules 22, 1932.
Siddiqui, B.S., Khatoon, N., Begum, S., Farooq, A.D., Qamar, K., Bhatti, H.A., Ali, S.K., 2012. Flavonoid and cardenolide glycosides and a pentacyclic triterpene from the leaves of *Nerium oleander* and evaluation of cytotoxicity. Phytochemistry 77, 238–244.
Wen, S., Chen, Y., Lu, Y., Wang, Y., Ding, L., Jiang, M., 2016. Cardenolides from the Apocynaceae family and their anticancer activity. Fitoterapia 112, 74–84.